IEEE Access
Multidisciplinary | Rapid Review | Open Access Journal

Received 25 May 2022, accepted 20 June 2022, date of publication 27 June 2022, date of current version 30 June 2022.

Digital Object Identifier 10.1109/ACCESS.2022.3186330

RESEARCH ARTICLE

Design of Robust PI Controllers for Interval Plants With Worst-Case Gain and Phase Margin Specifications in Presence of Multiple Crossover Frequencies

RADEK MATUŠŮ[1], BILAL ŞENOL[2], BARIS BAYKANT ALAGOZ[2], AND LIBOR PEKAŘ[3]

[1]Centre for Security, Information and Advanced Technologies (CEBIA–Tech), Faculty of Applied Informatics, Tomas Bata University in Zlín, 760 01 Zlín, Czech Republic
[2]Department of Computer Engineering, Faculty of Engineering, Inonu University, 44280 Malatya, Turkey
[3]Department of Automation and Control Engineering, Faculty of Applied Informatics, Tomas Bata University in Zlín, 760 01 Zlín, Czech Republic

Corresponding author: Radek Matušů (rmatusu@utb.cz)

ABSTRACT This article deals with the computation of robustly performing Proportional-Integral (PI) controllers for interval plants, where the performance measures are represented by the worst-case Gain Margin (GM) and Phase Margin (PM) specifications, in the event of multiple Phase Crossover Frequencies (PCFs) and/or Gain Crossover Frequencies (GCFs). The multiplicity of PCFs and GCFs poses a considerable complication in frequency-domain control design methods. The paper is a continuation of the authors' previous work that applied the robust PI controller design approach to a Continuous Stirred Tank Reactor (CSTR). This preceding application represented the system with a single PCF and a single GCF, but the current article focuses on a case of multiple PCFs and GCFs. The determination of a robust performance region in the P-I plane is based on the stability/performance boundary locus method and the sixteen plant theorem. In the illustrative example, a robust performance region is obtained for an experimental oblique wing aircraft that is mathematically modeled as the unstable interval plant. The direct application of the method results in the (pseudo-)GM and (pseudo-)PM regions that ''illogically'' protrude from the stability region. Consequently, a deeper analysis of the selected points in the P-I plane shows that the calculated GM and PM boundary loci are related to the numerically correct values, but that the results may be misleading, especially for the loci outside the stability region, due to the multiplicity of the PCFs and GCFs. Nevertheless, the example eventually shows that the important parts of the GM and PM regions, i.e., the parts that have an impact on the final robust performance region, are valid. Thus, the method is applicable even to unstable interval plants and to the control loops with multiple PCFs and GCFs.

INDEX TERMS Gain margin, interval plant, multiple crossover frequencies, oblique wing aircraft, phase margin, PI controllers, robust control, robust performance.

I. INTRODUCTION

Controlled systems with interval uncertainty, or just the interval plants, in short, represent a frequently used class of Linear Time-Invariant (LTI) mathematical models of the real controlled systems. The usage of these models may substitute the true complicated behavior of the systems, the inexact physical properties knowledge, or just the change of the parameters depending on various conditions. The well-known motivation for covering all modeling intricacies with the interval plant is that a group of linear robust analysis/synthesis methods may be used consequently.

The Proportional-Integral-Derivative (PID) controllers (and their special subtypes, such as PI controllers) remain

The associate editor coordinating the review of this manuscript and approving it for publication was Bo Pu.

without doubt alpha and omega of the control engineering practice. In the previous decades, many surveys and reports on a share of PID controllers at all practical control applications in various industry fields were presented [1]–[4]. The stated numbers usually vary between 90% and 98% of PID-based control loops, depending on the specific realm. It is not easy to find reliable and up-to-date statistical data, but the automatic control community estimates that PID controllers are used in more than 90% of industrial control applications even today [5]. Therefore, it still makes sense to investigate the tuning of PI(D) controllers, particularly under uncertain operating conditions. Consequently, it is reasonable that great attention has been paid to the research on robustly stabilizing or robustly performing PI(D) controllers for systems with parametric uncertainty [6], [7]. Frequently, the controlled systems are considered only as the interval plants, i.e., the LTI models with the independent structure of uncertainty and with the uncertainty bounding set in the shape of a (hyper-)box. These relatively simple models are commonly used for the description of much more complex real-world systems.

The problem of obtaining the nominal stability domains for control systems with PI(D) compensators was addressed by a number of researchers. Consequently, a series of methods was developed. For instance, the rigorous algorithm to identify the stability domain in the space of controller parameters, called D-decomposition, was invented as far back as 1948 by Neimark [8]. This efficient technique has become very popular, and thus the idea of D-decomposition was further developed and expanded not only by its inventor but also by many follow-up researchers – see, e.g. [9]–[15]. Among others, the parameter space approach, which is actually based on the concept of D-decomposition and which utilizes frequency sweeping, was presented in almost a classic book [12]. Apart from D-decomposition, other well-known methods in the field exist. For example, computation of PID stabilizers through the algorithms in which the frequency sweeping is parried by decoupling at singular frequencies is introduced in [16]. Another popular approach takes advantage of the generalized Hermite-Biehler theorem [17], [7]. The stability boundary locus method, which is a cornerstone of the extensions in this paper, was proposed in [18], [19]. Furthermore, it is worth also reminding some other works that present or compare various techniques for obtaining the stabilizing PI or PID controllers for time-delay-free as well as time-delay plants [20]–[30].

However, the practical control problems usually involve a degree of uncertainty, often parametric uncertainty. Hence, a natural step from the robust control viewpoint consists in extending the investigation of nominally stabilizing PI(D) controller parameters to the case of robustly stabilizing ones [31], [32]. A classic method that is used for making the nominally stabilizing methods applicable to robust stabilization of the interval plants is the sixteen plant theorem [33], [34]. Nevertheless, this elegant extreme-point-based tool holds true only if the first-order compensators (typically PI controllers) are considered. For the case of PID controllers, more general tools have to be employed, such as Kharitonov segments-based results [35]–[37].

Although stability represents the major requisite for functioning the control system, some performance is usually also requested. The Gain Margin (GM) and Phase Margin (PM) belong among the widely known measures of the control loop performance. The GM and PM can also be considered as gauges for so-called relative stability. Nominal stabilization of the plants for the specified GMs and PMs by means of the stability boundary locus method was published in [19], [38]. Further, the design of PI controllers for simultaneous achievement of the specified GM, PM, and Gain Crossover Frequency (GCF) by means of the curves in the GM-PM plane was presented in [39]. For some alternative techniques for mapping the performance requirements into the parameter space, see, e.g., [40]–[43].

Ensuring the performance under conditions of uncertainty, e.g., for all possible members of the interval plant family, leads to the term ''robust performance''. Naturally, the GM and PM can also be used in the robust performance framework [37], [44]–[47]. It was already shown in the literature [48], [7], [34] that the mentioned sixteen plant theorem is valid not only for the robust stability but is applicable also for the robust performance specifications in terms of GM and PM. For instance, the works [49], [50], [34] presented that the worst-case H_∞ norm is related to one of the sixteen Kharitonov plants. Furthermore, it was proved that the outer boundary of the Nyquist envelope of a stable, strictly proper interval plant is covered by the Nyquist plots of the sixteen Kharitonov plants [51], [52]. Although the entire Nyquist envelope does not generally come from the Kharitonov plants, the large and critical portions of the Nyquist envelope are covered by these Nyquist plots [51]. Consequently, the worst-case GM and PM of the feedback control system with the PI controller (generally a first-order controller) and an interval plant are deducible from its sixteen Kharitonov plants.

Usually, the uniqueness of Phase Crossover Frequencies (PCFs) and GCFs is supposed in frequency-domain control design methods, because their multiplicity poses a serious complication. For example, the paper [53] calls the multiplicity of crossover frequencies an Achilles heel of the analytical data-driven tuning procedures for control systems. However, this complicated situation may frequently appear in practice, and so there is a need for appropriate solutions.

This paper aims at the calculation of robustly performing PI controllers for interval plants with the worst-case GM and PM specifications with the special emphasis on the case of multiple PCFs and/or GCFs. This work further extends the applicability of the interesting generalization of the stability boundary locus method for specified GM and PM, which was introduced in [19], [38] and applied to the fixed-parameter controlled plants. In the authors' previous work [54], the set of robustly performing PI controllers was calculated for a Continuous Stirred Tank Reactor (CSTR), assumed as

the stable interval plant, by combining the technique from [19], [38] with the sixteen plant theorem. The current paper is intended as a follow-up to the paper [54], and it focuses on the case with multiple PCFs and GCFs. The technique is applied to the mathematical model of an experimental oblique wing aircraft [34], [55], [35], which is supposed to be in the form of an interval plant. The members of the considered interval plant family may be both stable and unstable systems. In the illustrative example, the computation of a robust performance region in the P-I plane for given GM and PM specifications is discussed to a great extent.

The remainder of this paper is structured as follows. The stability boundary locus method and its application to obtain the robust stability or robust performance regions in the P-I plane for the control loops with interval plants are summarized in Section II. Then, the issues of the systems with multiple PCFs and GCFs are outlined in Section III. Further, the specific example of the oblique wing aircraft model, which leads to multiple PCFs and GCFs, is analyzed in the extensive Section IV. The final Section V offers some concluding remarks.

II. ROBUST STABILITY AND ROBUST PERFORMANCE OF FEEDBACK LOOPS WITH PI CONTROLLER AND INTERVAL PLANT

Consider the feedback control loop with an interval plant $G(s, a, b)$, the PI controller $C(s)$, and virtual gain-phase margin tester $Me^{-j\theta}$, where M and θ are subject to GM and PM specifications [37], [44], [47]. This closed-loop system is depicted in Fig. 1. Note that for $M = 1$ and $\theta = 0$, an ordinary feedback connection is obtained.

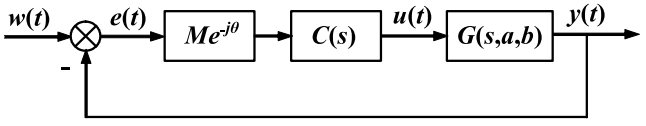

FIGURE 1. Feedback control loop with an interval plant and gain-phase margin tester.

The signals from Fig. 1 have the following meaning: $w(t)$ represents the reference signal, $e(t)$ is the control (tracking) error, $u(t)$ stands for control (actuating) signal, and $y(t)$ symbolizes the controlled (output) signal. Further, $C(s)$ denotes a conventional PI controller given by:

$$C(s) = P + \frac{I}{s} = \frac{Ps + I}{s} \tag{1}$$

and $G(s, a, b)$ represents a strictly proper interval plant:

$$G(s, b, a) = \frac{B(s, b)}{A(s, a)} = \frac{\sum_{i=0}^{m} \left[b_i^-, b_i^+\right] s^i}{s^n + \sum_{i=0}^{n-1} \left[a_i^-, a_i^+\right] s^i}, \quad m < n \tag{2}$$

with superscripts "$-$" and "$+$" symbolizing the lower and upper bounds of the relevant parameters, respectively.

It is the well-known fact that a first-order controller (such as PI controller (1)) robustly stabilizes the interval plant (2) if and only if it stabilizes every single Kharitonov plant [33], [34], and that there are sixteen of these Kharitonov plants, given by the variations:

$$G_{k,l}(s) = \frac{B_k(s)}{A_l(s)}, \quad k, l \in \{1, 2, 3, 4\} \tag{3}$$

where polynomials from $B_1(s)$ to $B_4(s)$ are the Kharitonov polynomials [56] of the numerator $B(s, b)$ of (2), i.e.:

$$\begin{aligned} B_1(s) &= b_0^- + b_1^- s + b_2^+ s^2 + b_3^+ s^3 + \cdots \\ B_2(s) &= b_0^+ + b_1^+ s + b_2^- s^2 + b_3^- s^3 + \cdots \\ B_3(s) &= b_0^+ + b_1^- s + b_2^- s^2 + b_3^+ s^3 + \cdots \\ B_4(s) &= b_0^- + b_1^+ s + b_2^+ s^2 + b_3^- s^3 + \cdots \end{aligned} \tag{4}$$

and polynomials $A_1(s)$ to $A_4(s)$ are the analogous Kharitonov polynomials of the denominator $A(s, a)$ of (2).

Nevertheless, it was shown that this extreme-based sixteen plant principle is applicable also for satisfying the performance specifications, such as GMs and PMs [48], [7], [34], [49]–[54]. Thus, the worst-case GMs and PMs for the feedback control system (Fig. 1) with a first-order (PI) controller (1) and a strictly proper interval plant (2) may be calculated by means of GMs and PMs for the PI control loops with the sixteen Kharitonov plants.

All in all, the problem of computation of robustly stabilizing or robustly performing PI controller for an interval plant can be transformed in the set of sixteen simpler problems of computation of stabilizing or performing PI controller for the Kharitonov plants.

This partial task may be solved by using a relatively simple but effective technique that is based on plotting the stability boundary locus or performance boundary locus in the P-I plane [18], [19].

Assume a plant given by a conventional fixed-parameter transfer function, where s is substituted with $j\omega$, and where the numerator and denominator polynomials are decomposed into their even (subscripts "E") and odd (subscripts "O") parts:

$$G(j\omega) = \frac{B_E(-\omega^2) + j\omega B_O(-\omega^2)}{A_E(-\omega^2) + j\omega A_O(-\omega^2)} \tag{5}$$

In the works [18], [19], the parametric equations for calculating the stability boundary locus in the P-I plane were derived as:

$$\begin{aligned} P(\omega) &= \frac{X_5(\omega)X_4(\omega) - X_6(\omega)X_2(\omega)}{X_1(\omega)X_4(\omega) - X_2(\omega)X_3(\omega)} \\ I(\omega) &= \frac{X_6(\omega)X_1(\omega) - X_5(\omega)X_3(\omega)}{X_1(\omega)X_4(\omega) - X_2(\omega)X_3(\omega)} \end{aligned} \tag{6}$$

where

$$\begin{aligned} X_1(\omega) &= -\omega^2 B_O(-\omega^2) \\ X_2(\omega) &= B_E(-\omega^2) \\ X_3(\omega) &= \omega B_E(-\omega^2) \end{aligned}$$

$$X_4(\omega) = \omega B_O(-\omega^2)$$
$$X_5(\omega) = \omega^2 A_O(-\omega^2)$$
$$X_6(\omega) = -\omega A_E(-\omega^2) \quad (7)$$

The corresponding parametric curve, together with the $I = 0$ line, divides the P-I plane into the stability and instability areas. The related sub-problems of the decision on stable/unstable areas via choosing the test points and a convenient frequency ω gridding by means of the Nyquist plot-based technique [20] are also discussed in [18], [19].

The same above-mentioned principle may be used for obtaining the performance boundary locus for selected GMs or/and PMs. In this case, the relations (7) are generalized to [19]:

$$X_1(\omega) = M\left(\omega B_E(-\omega^2)\sin\theta - \omega^2 B_O(-\omega^2)\cos\theta\right)$$
$$X_2(\omega) = M\left(B_E(-\omega^2)\cos\theta + \omega B_O(-\omega^2)\sin\theta\right)$$
$$X_3(\omega) = M\left(\omega B_E(-\omega^2)\cos\theta + \omega^2 B_O(-\omega^2)\sin\theta\right)$$
$$X_4(\omega) = M\left(\omega B_O(-\omega^2)\cos\theta - B_E(-\omega^2)\sin\theta\right)$$
$$X_5(\omega) = \omega^2 A_O(-\omega^2)$$
$$X_6(\omega) = -\omega A_E(-\omega^2) \quad (8)$$

The choice $\theta = 0$ leads to the performance boundary locus for a requested GM M. On the other hand, the performance boundary locus for a selected PM θ can be obtained under the assumption that $M = 1$ (not 0, as was mistakenly stated in [54]). Once both GM and PM performance regions are determined on the basis of the obtained boundary loci, their intersection defines the performance region that guarantees the requested GM and PM together.

Consequently, as stated hereinbefore, the final robust performance region for an interval plant can be obtained as the intersection of sixteen ''partial'' performance regions for the sixteen Kharitonov plants.

The application of the principle has already been demonstrated on robust PI controller design for a CSTR in the authors' previous work [54]. However, this paper focuses on a special case of multiple PCFs and GCFs.

III. MULTIPLE PHASE AND GAIN CROSSOVER FREQUENCIES

The elementary principle of GM and PM is very well known from the classical control theory. The GM and PM values can be considered as the safety margins before a closed-loop system becomes unstable (or marginally stable, to be more precise). The determination of the GM and PM values, valid for a closed-loop system, is based on a relevant open-loop system. In some specific cases, the GM and PM may not be enough to indicate the true robustness of a system when the gain and phase are varying simultaneously [57]. Nevertheless, in the majority of common control systems, the GM and PM are good indicators of the system's robustness. The exact definitions and the basic graphical representations of GM and PM via Nyquist or Bode plots can be found in many (robust) control books.

However, as noted in [58], an array of literature sources stay only halfway in explaining GM and PM. They usually limit their attention to the case of a stable open-loop system with the Nyquist curve crossing the negative real axis on the right-hand side of the critical point $[-1, 0j]$, and crossing the unit circle below the real axis (usually in the third quadrant). Remind that also the open-loop systems with zero poles (integrators) are considered as stable ones from the viewpoint of the Nyquist stability criterion. Alternatively, the elucidation may be supported by the corresponding Bode diagrams. Anyway, such a scenario then corresponds to a stable closed-loop system with the GM $M > 1(= 0$ dB) and the PM $\theta > 0°$. Nonetheless, the situation may be much more complicated.

The special cases include infinite GM and/or infinite PM. It means that regardless of the size of GM and/or PM, the closed-loop control system remains always stable.

A typical counterexample to the classic academic example from the majority of (robust) control books appears when the open-loop Nyquist plot crosses the negative real axis on the left-hand side of the point $[-1, 0j]$, and crosses the unit circle above the real axis. This emerges, e.g., in the case of an unstable open loop (with a single unstable pole) and a stable closed loop. Then, the GM $M < 1(= 0$ dB) and the PM $\theta < 0°$ are observed. Consequently, the closed-loop system stability will be endangered by decreasing the gain or increasing the phase.

However, the situation can be even more complex. For example, the Nyquist curve may cross the negative real axis on both the right-hand side and the left-hand side of the point $[-1, 0j]$, and/or it may cross the unit circle both below and above the real axis. In such an event, GM and/or PM are given by the intervals, i.e., by the minimum and maximum GM/PM. The graphical representation of these both-side crossovers can be found, e.g., in Figure 9.13 in the book [57], which is one of not many sources that also examines this eventuality.

The most general case then supposes more crossings on both mentioned sides for GM and/or PM. In such a situation, the nearest crossing to the critical point $[-1, 0j]$ and/or the nearest crossing to the real axis are taken as the significant ones. The multiplicity of PCFs and GCFs means a considerable complication in frequency-domain control design methods. As stated in Introduction, the work [53] calls it an Achilles heel of the analytical data-driven tuning procedures for control systems. Thus, these complex cases with multiple PCFs and GCFs need increased attention.

The following example analyzes the application of the method for calculation of robustly performing PI controllers to the interval plant under prescribed worst-case GM and PM specifications in the event of multiple PCFs and GCFs.

IV. ILLUSTRATIVE EXAMPLE – OBLIQUE WING AIRCRAFT MODEL

A. MATHEMATICAL MODEL AND PROBLEM FORMULATION

Assume the mathematical model of an experimental oblique wing aircraft, which is given by the interval plant, adopted from [34] with the original cited reference to [55]:

$$G(s,b,a)=\frac{b_1 s+b_0}{s^4+a_3 s^3+a_2 s^2+a_1 s+a_0} \tag{9}$$

where the parameters may lie within the following intervals:

$$\begin{aligned} b_1 &\in [54,\ 74]\\ b_0 &\in [90,\ 166]\\ a_3 &\in [2.8,\ 4.6]\\ a_2 &\in [50.4,\ 80.8]\\ a_1 &\in [30.1,\ 33.9]\\ a_0 &\in [-0.1,\ 0.1] \end{aligned} \tag{10}$$

Note that the interval plant family (9) contains stable as well as unstable members.

The objective is to find the region of parameters of the PI controller (1) that lead to the feedback control loop (Fig. 1) with a minimum GM $M = 2(\approx 6$ dB) together with a minimum PM $\theta = 30°$ for all possible interval plant parameters (10).

B. PRELIMINARY ANALYSIS

As it was shown in [54] and described in the previous Section 2, the robust performance region can be obtained as the intersection of sixteen GM regions and sixteen PM regions that are plotted for sixteen Kharitonov plants (3). It is still valid, but the situation can be a bit trickier for the cases of multiple PCFs and/or GCFs.

Focus, e.g., on the Kharitonov plant $G_{1,2}(s)$:

$$\begin{aligned} G_{1,2}(s)=\frac{B_1(s)}{A_2(s)}&=\frac{b_1^- s+b_0^-}{s^4+a_3^- s^3+a_2^- s^2+a_1^+ s+a_0^+}\\ &=\frac{54s+90}{s^4+2.8s^3+50.4s^2+33.9s+0.1} \end{aligned} \tag{11}$$

For this plant, the transfer function (5) has the specific even and odd parts of the numerator and denominator polynomials as follows:

$$\begin{aligned} B_E(-\omega^2)&=90\\ B_O(-\omega^2)&=54\\ A_E(-\omega^2)&=\omega^4+50.4(-\omega^2)+0.1\\ A_O(-\omega^2)&=2.8(-\omega^2)+33.9 \end{aligned} \tag{12}$$

The stability boundary locus can be obtained by simultaneous solution of (6) and (7) for a range of nonnegative frequencies ω, combined with the $I = 0$ line. Then, the performance boundary locus (i.e., the GM boundary locus or the PM boundary locus) can be determined by using (6) and (8), together with the $I = 0$ line.

The stability boundary locus is depicted by the black curve in Fig. 2. It can be easily verified that the interior of the obtained black shape defines the stability region. Then, in the same figure, the red curve corresponds to the (pseudo-)GM boundary locus for $M = 2(\approx 6$ dB), and the blue curve presents the (pseudo-)PM boundary locus for $\theta = 30°$. Again, the insides of these shapes, calculated according to (6) and (8), give the corresponding performance regions.

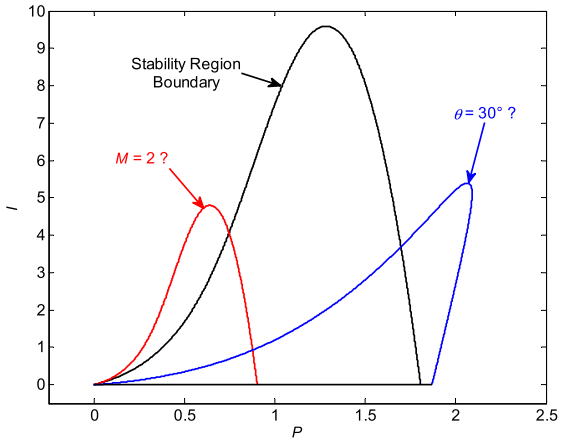

FIGURE 2. Stability region boundary, (pseudo-)GM region boundary ($M = 2$ (≈ 6 dB)), and (pseudo-)PM region boundary ($\theta > 30°$) obtained using (6)-(8) for the Kharitonov plant (11).

However, a specific phenomenon can be observed in Fig. 2. The (pseudo-)GM region and the (pseudo-)PM region protrude from the stability region, which makes no sense at first sight. Thus, the true GM and PM will be analyzed in 11 chosen interesting points ($p_1 - p_{11}$) that were selected as shown in Fig. 3.

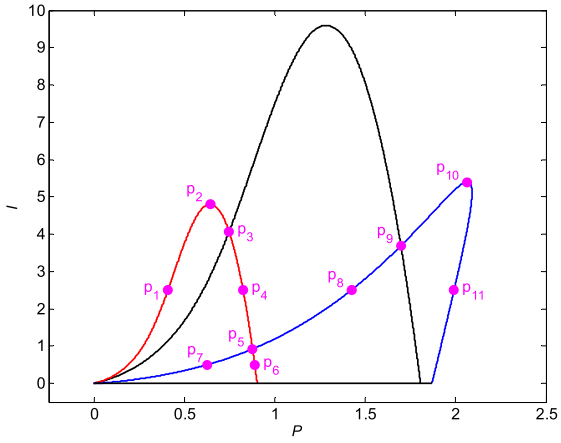

FIGURE 3. Position of 11 analyzed points in the PI plane.

C. DETAILED ANALYSIS IN 11 SELECTED POINTS

The GM and PM will be successively analyzed for the control loop with the Kharitonov plant (11) and 11 pairs of PI controller parameters that correspond to 11 points in the P-I

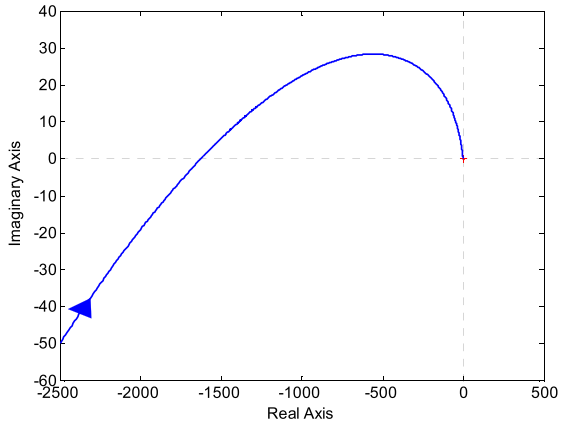

FIGURE 4. The Nyquist diagram for the point p_1 (the full view).

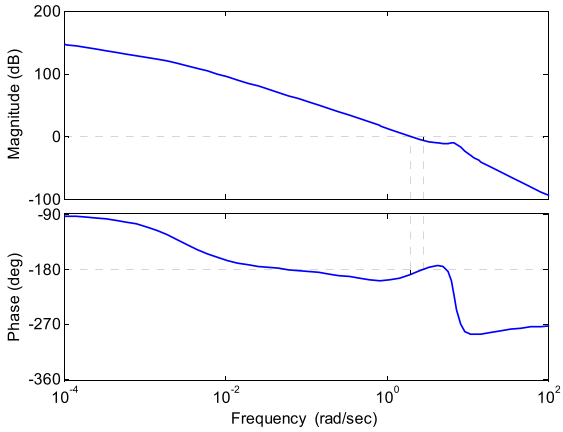

FIGURE 6. The Bode diagram for the point p_1.

plane (Fig. 3). The GM/PM data will be based on the results obtained by using the standard Matlab "allmargin" function.

1) POINT 1

The first selected point p_1 corresponds to the parameters $P = 0.4093$, $I = 2.5$. As can be seen, it lies on the obtained GM boundary locus for $M = 2(\approx 6\,\text{dB})$, but at the same time, it is located outside the stability region. So what is wrong? The answer resides in the multiplicity of the PCFs, because the control loop has three pseudo-GM values 6.1492×10^{-4}, 2, 3.5206 [−], which occur at the PCFs 0.0639, 2.8519, 5.5385 [rad/s], respectively. Besides, there is the pseudo-PM -8.2530 [°] at the GCF 1.9688 [rad/s]. The whole situation can be clarified by means of the Nyquist and Bode diagrams of the open-loop system. Fig. 4 shows the (the full view) Nyquist diagram (for the positive frequencies), and Fig. 5 adds a closer look near the critical point $[-1, 0j]$. The horizontal axis, labeled as "Real Axis", represents the real parts of the open-loop sinusoidal transfer function $L(j\omega) = C(j\omega)G_{1,2}(j\omega)$, and the vertical axis, labeled as "Imaginary Axis" represents the imaginary parts of the open-loop sinusoidal transfer function $L(j\omega)$. The same notation is also used in all the following relevant figures. Then, Fig. 6 presents the Bode diagram.

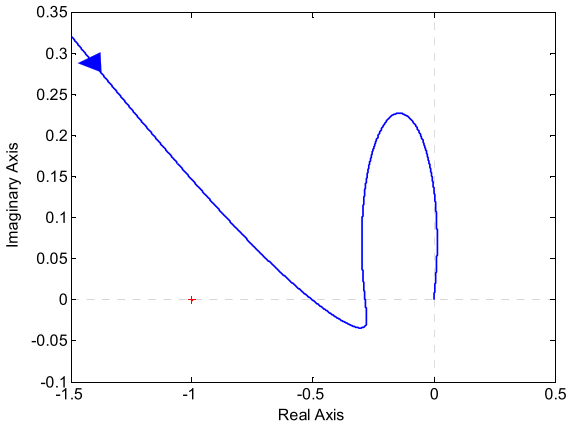

FIGURE 5. The Nyquist diagram for the point p_1 (a detailed view).

Thus, Figs. 4-6 demonstrate that the middle value 2 of three pseudo-GMs may be calculated, but it has no practical meaning in this case since the closed-loop control system is unstable in fact.

2) POINT 2

The second chosen point p_2 ($P = 0.6427$, $I = 4.7968$) leads to three pseudo-GMs 3.0777×10^{-4}, 1.5469, 1.9997, occurring at the PCFs 0.0626, 3.6287, 4.9067, respectively. Moreover, there is the pseudo-PM -4.9267 at the GCF 2.7358. The shapes of the Nyquist and Bode diagrams are very similar to the previous case (point 1), so only a zoomed-view Nyquist plot and Bode plot are shown in Figs. 7 and 8, respectively.

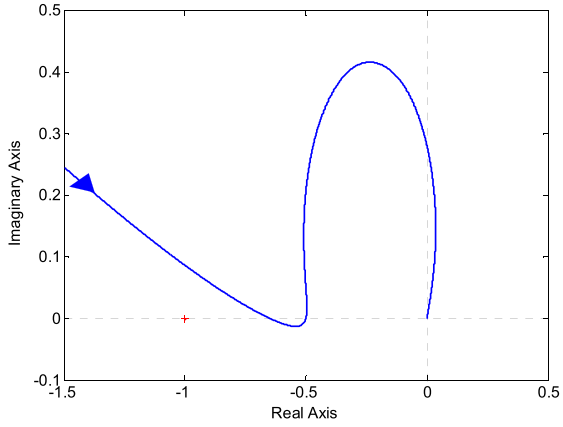

FIGURE 7. The Nyquist diagram for the point p_2 (a detailed view).

Again, it can be seen that the pseudo-GM with the value 2 has no meaning at all here. There is even one smaller pseudo-GM from the right-hand side (Fig. 7), but even this one is practically useless due to the instability of the closed-loop control system.

3) POINT 3

The crossing of the GM boundary locus and the stability boundary locus was chosen as the third point p_3

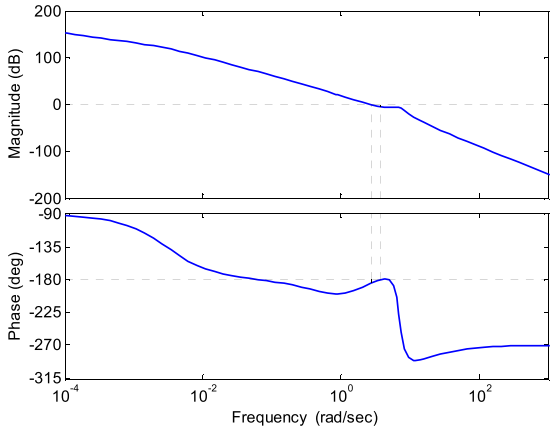

FIGURE 8. The Bode diagram for the point p_2.

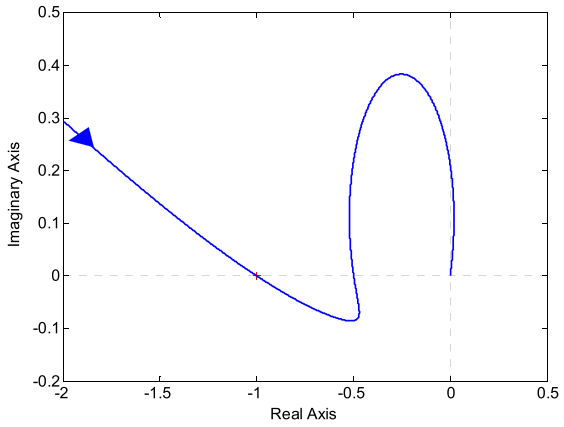

FIGURE 9. The Nyquist diagram for the point p_3 (a detailed view).

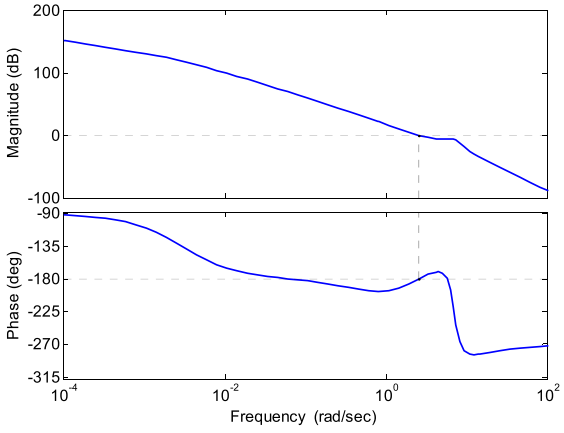

FIGURE 10. The Bode diagram for the point p_3.

($P = 0.7474, I = 4.0676$). For p_3, there are three GM candidates 3.8876×10^{-4}, 1.0001, 2.0001 at PCFs 0.0648, 2.5584, 5.7456, respectively, and the PM 5.4083×10^{-4} at GCF 2.5584. The basic shape of the Nyquist curve is similar to the previous cases, and thus only its zoomed version is provided (Fig. 9). Further, the Bode diagram is depicted in Fig. 10.

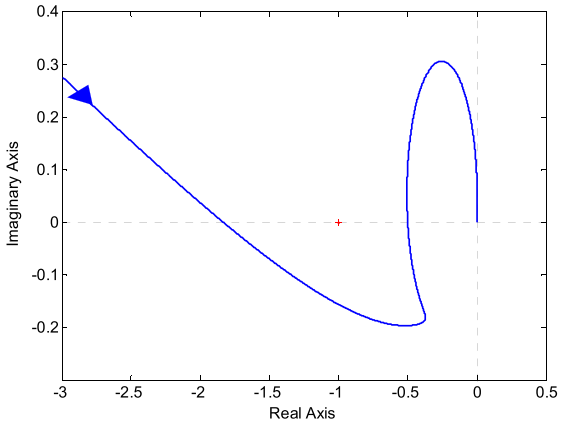

FIGURE 11. The Nyquist diagram for the point p_4 (a detailed view).

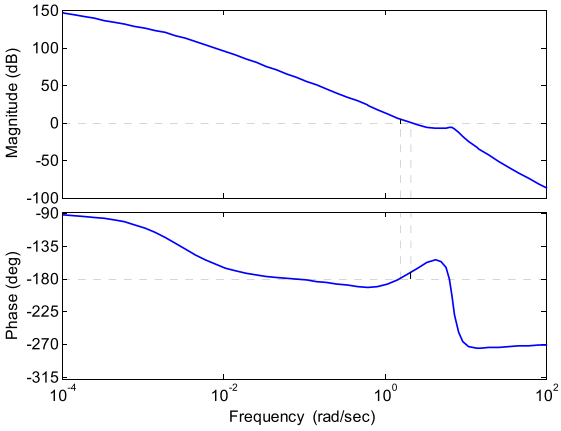

FIGURE 12. The Bode diagram for the point p_4.

In this scenario, the closed-loop control system is marginally stable, i.e., it is on the stability border (the true GM is 1.0001 and the true PM is 5.4083×10^{-4}), which concurs with the position of p3 in the P-I plane (Fig. 3).

4) POINT 4

The fourth selected point p_4 with coordinates $P = 0.8252, I = 2.5$ results in three GM candidates 7.9997×10^{-4}, 0.5462, 2.0001 at PCFs 0.0728, 1.5436, 6.3174, respectively, and the PM 9.0438 at GCF 2.1114. A zoomed Nyquist diagram and the Bode diagram are shown in Fig. 11 and Fig. 12, respectively.

As can be seen, the closed-loop control system is stable. Moreover, it can be observed that this is the first time when the value of GM 2 is of practical importance. It serves as the right-hand side stability margin (Fig. 11). Despite the fact that the instability may also be reached from the left-hand side (see Fig. 9), because the true GM is given by the interval [0.5462, 2.0001], the number 2 represents the relevant GM-related value now.

5) POINT 5

The crossing of the GM boundary locus and the PM boundary locus was set as the fifth point p_5 ($P = 0.8775, I = 0.922$).

This interesting point corresponds to the GM 2 at the PCF 6.6794 and the PM 30.0038 at the GCF 1.6109. The Nyquist diagram is plotted in Fig. 13. Note that it is not a zoomed version but a full one because there are no more imaginary axis crossings on the left-hand side. Then, the Bode diagram is shown in Fig. 14.

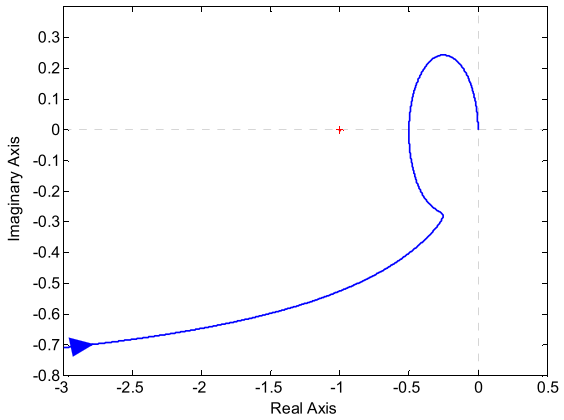

FIGURE 13. The Nyquist diagram for the point p_5.

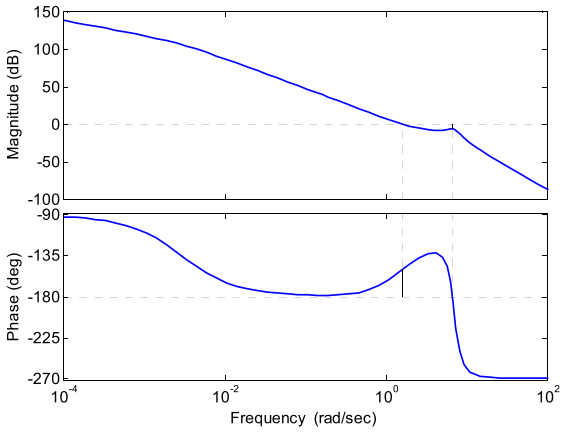

FIGURE 14. The Bode diagram for the point p_5.

Thus, at the point p_5, the closed-loop control system is stable, and both GM and PM values are exactly at the minimum requested levels.

6) POINT 6

The sixth chosen point p_6 is located at the GM boundary locus and inside the PM region simultaneously ($P = 0.8895, I = 0.5$). The corresponding control loop has the GM 2 at the PCF 6.7611 and the PM 42.2626 at the GCF 1.492. The Nyquist and Bode plots (very similar to the previous point p_5) are depicted in Figs. 15 and 16, respectively.

As can be seen, for the point p_6, the closed-loop control system is stable, the minimum acceptable value of GM and the higher than requested value of PM were obtained.

7) POINT 7

The coordinates of the seventh point p_7 were selected as $P = 0.6272, I = 0.5$, which means p_7 lies on the PM boundary

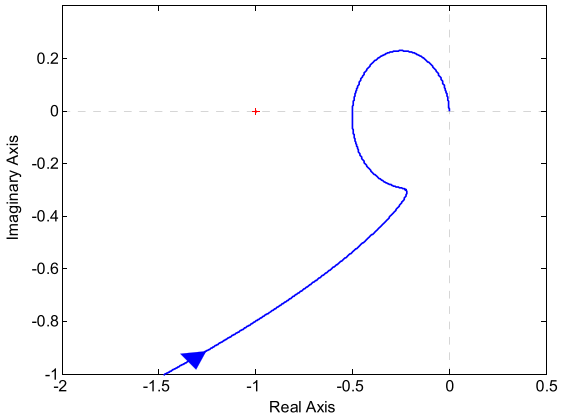

FIGURE 15. The Nyquist diagram for the point p_6.

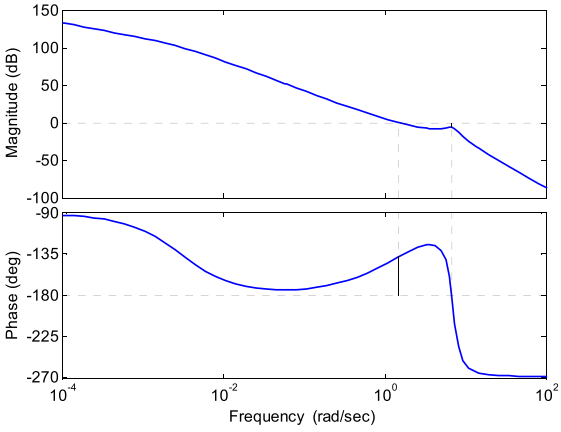

FIGURE 16. The Bode diagram for the point p_6.

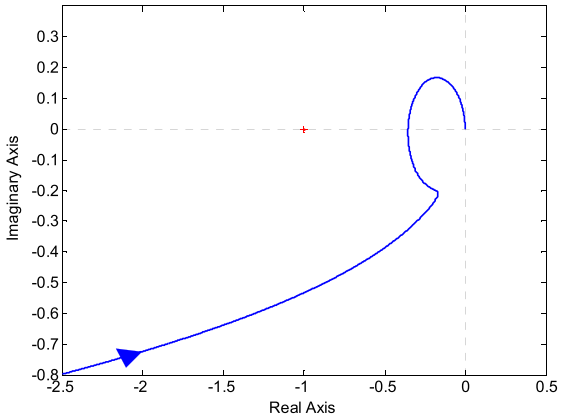

FIGURE 17. The Nyquist diagram for the point p_7.

locus and inside the GM region. This case leads to the GM 2.8182 at the PCF 6.7224 and the PM 29.9978 at the GCF 1.2411. The Nyquist and Bode diagrams (again, very similar to the previous two points) are plotted in Figs. 17 and 18, respectively.

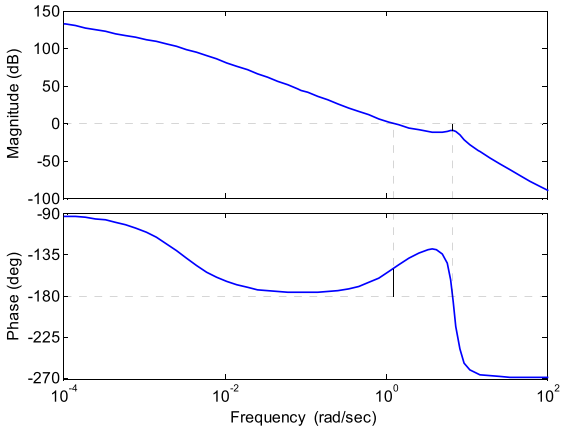

FIGURE 18. The Bode diagram for the point p_7.

As expected, the closed-loop control system is stable, and it has the minimum requested value of PM and the higher than requested value of GM.

8) POINT 8

The eighth point p_8 ($P = 1.4251, I = 2.5$) results in three GM candidates 0.0014, 0.1358, 1.2065 at the PCFs 0.0970, 0.8497, 6.5583, respectively, and the PM 30.0019 at the GCF 2.5251. A zoomed Nyquist diagram (with one more imaginary axis crossing on the left-hand side in the full view) and the Bode diagram are presented in Figs. 19 and 20, respectively.

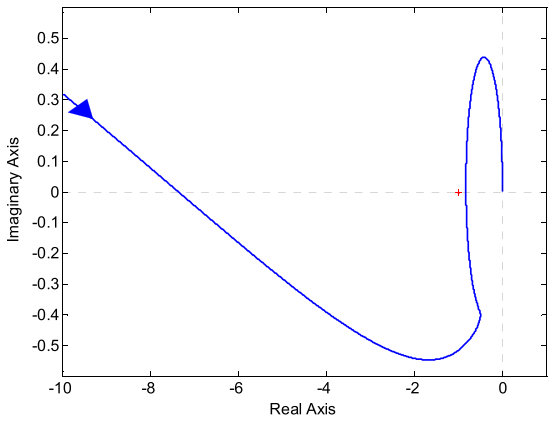

FIGURE 19. The Nyquist diagram for the point p_8 (a detailed view).

For the point p_8, the closed-loop control system is stable. The GM is given by the interval [0.1358, 1.2065], and the minimum requested value of PM is obtained, which is in compliance with the position of p_8 in the P-I plane.

9) POINT 9

The crossing of the PM boundary locus and the stability boundary locus is a position of the ninth chosen point p_9 ($P = 1.6977, I = 3.6822$). In this case, there are three candidates for the GM 7.1261×10^{-4}, 0.1726, 1 at the

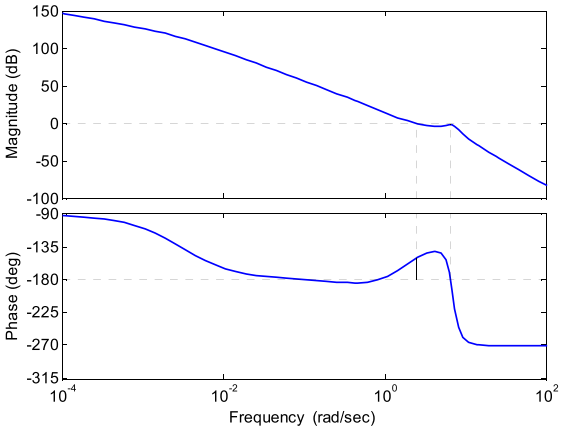

FIGURE 20. The Bode diagram for the point p_8.

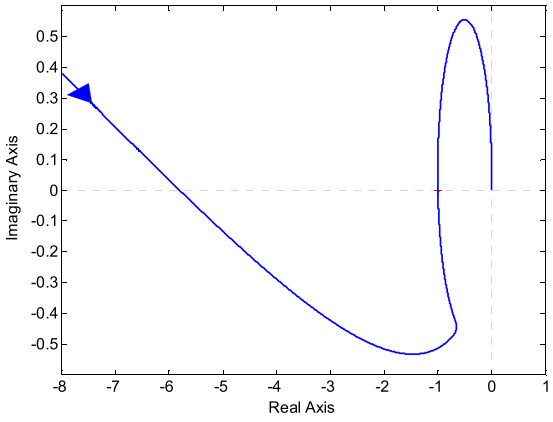

FIGURE 21. The Nyquist diagram for the point p_9 (a detailed view).

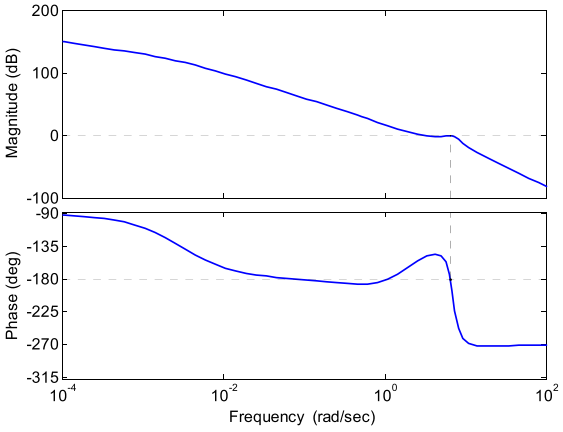

FIGURE 22. The Bode diagram for the point p_9.

PCFs 0.0834, 1.1119, 6.4832, respectively, and three PM candidates 30.0030, −0.1633, −11.9730 at the GCFs 3.1100, 6.4870, 6.7399. The zoomed version of the Nyquist curve (with one more imaginary axis crossing on the left-hand side in the full scale) is provided in Fig. 21, and the Bode plots are shown in Fig. 22.

For the point p_9, the closed-loop control system is marginally stable (on the stability border), which concurs with the position of p_9 in the P-I plane (Fig. 3). Thus, the true GM is 1 and the true PM is near 0 (the value -0.1633 was computed). As can be seen, the pseudo-PM with the requested value 30 was theoretically calculated as one of the obtained values, but it has no practical meaning in this case.

10) POINT 10

The tenth selected point p_{10} ($P = 2.0652, I = 5.3968$) corresponds to a trio of the pseudo-GM values 4.0964×10^{-4}, 0.1840, 0.8105, which occur at the PCFs 0.0766, 1.3454, 6.3989, respectively, and a trio of the pseudo-PM values 29.9992, 28.7164, -45.7744 at the GCFs 4.4945, 4.8948, 7.3648, respectively. A detailed view of the Nyquist diagram (with one more imaginary axis crossing on the left-hand side in the full view) is given in Fig. 23, and the Bode diagram is depicted in Fig. 24.

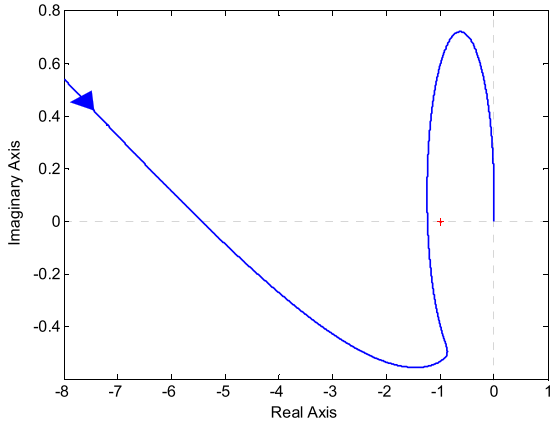

FIGURE 23. The Nyquist diagram for the point p_{10} (a detailed view).

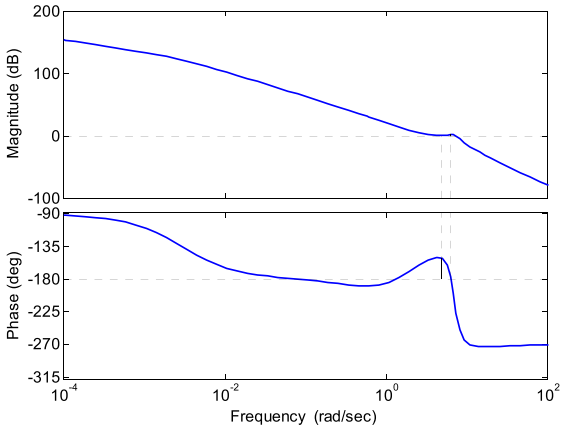

FIGURE 24. The Bode diagram for the point p_{10}.

Obviously, although one of the calculated pseudo-PM values has the requested level, it has no practical meaning here. The closed-loop control system is unstable.

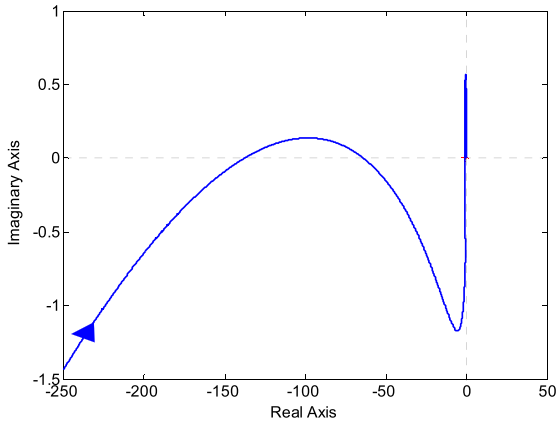

FIGURE 25. The Nyquist diagram for the point p_{11} (the full view).

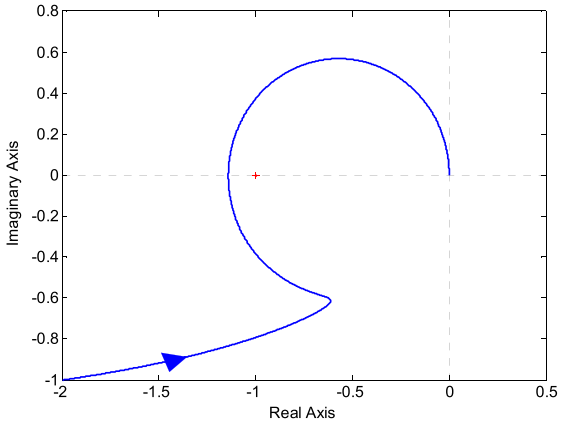

FIGURE 26. The Nyquist diagram for the point p_{11} (a detailed view).

11) POINT 11

The last chosen point p_{11} ($P = 1.9907, I = 2.5$) leads to three pseudo-GMs 0.0073, 0.0157, 0.8765, occurring at the PCFs 0.2175, 0.3163, 6.6455, respectively, and three pseudo-PMs 43.6417, 30.0058, -28.5065 at the GCFs 3.2510, 5.7969, 7.2051. Fig. 25 shows the Nyquist diagram in the full view, and Fig. 26 brings a nearer look to the neighborhood of the critical point $[-1, 0j]$. Finally, Fig. 27 depicts the Bode plots.

Similarly to the previous point p_{10}, a calculated value of the pseudo-PM 30 is meaningless also here, for the point p_{11}. In fact, the closed-loop control system is unstable.

D. ANALYSIS SUMMARY

The numerical results from the preceding analysis are briefly summarized in Table 1. It contains all data obtained by means of Matlab "allmargin" function, i.e., including pseudo-GMs and pseudo-PMs. The true GMs and PMs are highlighted by the blue color. Moreover, the values of the requested worst-case GM 2 and PM 30 are highlighted by the **bold font**.

The numerical results from the preceding analysis are briefly summarized in Table 1.

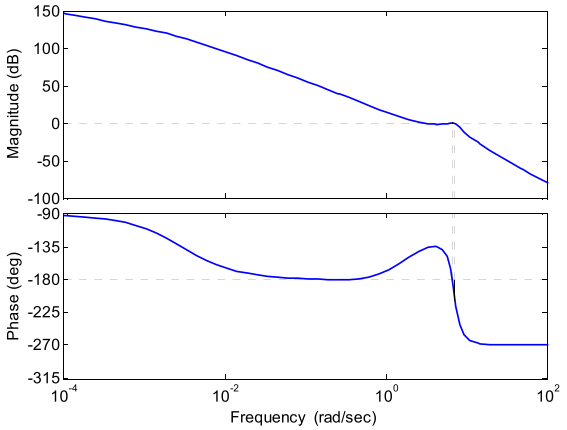

FIGURE 27. The Bode diagram for the point p_{11}.

TABLE 1. Gain margin and phase margin values for 11 selected points in the P-I plane (Fig. 3).

Point	Gain Margins (Pseudo and True)	Phase Margins (Pseudo and True)	S/U/MS*
p_1	6.1492x10^{-4}, **2**, 3.5206	-8.2530	U
p_2	3.0777x10^{-4}, 1.5469, **1.9997**	4.9267	U
p_3	3.8876x10^{-4}, 1.0001, **2.0001**	5.4083x10^{-4}	MS
p_4	7.9997x10^{-4}, 0.5462, **2.0001**	9.0438	S
p_5	**2**	**30.0038**	S
p_6	**2**	42.2626	S
p_7	2.8182	**29.9978**	S
p_8	0.0014, 0.1358, 1.2065	**30.0019**	S
p_9	7.1261x10^{-4}, 0.1726, 1	**30.0030**, -0.1633, -11.9730	MS
p_{10}	4.0964x10^{-4}, 0.1840, 0.8105	**29.9992**, 28.7164, -45.7744	U
p_{11}	0.0073, 0.0157, 0.8765	43.6417, **30.0058**, -28.5065	U

*Closed-Loop System Stability (S=Stable, U=Unstable, MS=Marginally Stable)

Apparently, the algorithm (6), (8) produces the performance boundary loci that are related to the "numerically correct" requested values of GM and/or PM, even for the case of multiple crossover frequencies. However, the obtained results may be misleading, especially for the loci outside the stability region, where the calculated values are meaningless. Nevertheless, even inside the stability region, the determination of the GM or PM may be complicated in the case of multiple crossover frequencies since there may be margins for both increasing and decreasing gain/phase. Fortunately, it seems the computed values inside the stability region, and especially inside the performance region, make sense and have significance for robust controller design. All in all, the intersection of the GM region and the PM region (Fig. 2) defines the relevant performance region, in which both minimum required GM and minimum required PM are fulfilled.

The analysis was accomplished for the Kharitonov plant $G_{1,2}(s)$ (11), but similar findings would also be obtained for other Kharitonov plants, even for the unstable ones.

E. ROBUST PERFORMANCE REGION

The final robust performance region can be obtained as the intersection of sixteen partial performance regions for each

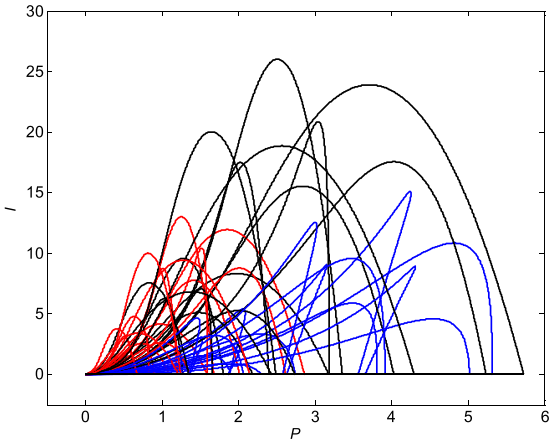

FIGURE 28. GM regions (red), PM regions (blue), and stability regions (black) for all sixteen Kharitonov plants (3) of (9).

of the sixteen Kharitonov plants (3). Thus, it may be practically achieved as the intersection of sixteen GM regions and sixteen PM regions [54].

Fig. 28 shows the set of sixteen GM regions (plotted by using the red curves), PM regions (plotted by means of the blue curves), and also the stability regions (depicted by the black curves), just for completeness.

The intersection of all GM and PM regions from Fig. 28 defines the final robust performance controller design region. This robust performance region is moved closer and indicated by the yellow area in Fig. 29.

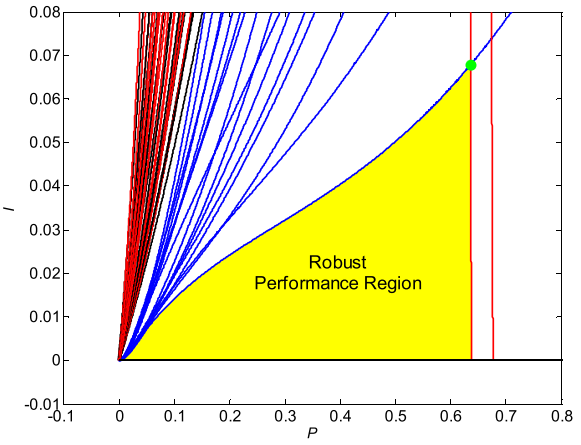

FIGURE 29. Robust performance region for the interval plant (9).

As summary, the PI controllers (1) with parameters inside the robust performance region in the P-I plane (Fig. 29) guarantee the stable feedback control loop with the GM greater than 2 (≈6 dB) and the PM greater than 30° for all possible parameters (10) of the interval plant (9), which represents a mathematical model of an experimental oblique wing aircraft. Obviously, if a pair of P-I parameters is located on the border of the robust performance region, one or both of the performance measures will be exactly at the minimum

requested worst-case levels. A reasonable choice of the controller corresponds to the exact GM 2 (≈6 dB) and the exact PM 30° for a worst-case member of the interval plant family (and the higher values of GM and PM for the remaining members). This controller is given by the upper right vertex of the robust performance region from Fig. 29 (marked by the green point), i.e., its parameters are $P = 0.6359$, $I = 0.0678$.

This example reveals a practical benefit that this graphical design methodology can easily cope with a difficult robust controller design problem that requires the preservation of the control performance within the predefined parametric uncertainty ranges of the controlled system.

V. CONCLUSION

The article was focused on the calculation of robustly performing PI controllers for interval plants under given worst-case GM and PM design specifications with stress on the case of multiple PCFs and/or GCFs. It was intended as a follow-up to the authors' previous work [54], which extended the stability boundary locus method for specified GM and PM and for fixed-parameter plants presented in [19], [38] by combining it with the sixteen plant theorem. In the paper [54], the approach was applied to a CSTR, modeled as the stable interval plant, which led to the case of a control loop with a unique PCF and GCF. The current paper concentrated on the control systems with multiple crossover frequencies.

The method was utilized for obtaining the robust performance region in the P-I plane for an experimental oblique wing aircraft, mathematically modeled as the unstable interval plant. The straightforward application of the technique led to the (pseudo-)GM and (pseudo-)PM regions that protruded from the stability region, which had no sense. Consequently, a deeper analysis of the selected points in the P-I plane showed the fact that the calculated GM and PM boundary loci were related to the numerically correct values; however, the analysis also demonstrated that the results might be misleading, especially for the loci outside the stability region, due to the multiplicity of the PCFs and/or GCFs. Nonetheless, the example showed that the important parts of the GM and PM regions that had an impact on the final robust performance region were valid, and thus the method might be applicable even to unstable interval plants and to the control loops with multiple crossover frequencies.

REFERENCES

[1] K. J. Åström and T. Hägglund, *PID Controllers: Theory, Design, and Tuning*, 2nd ed. Research Triangle Park, NC, USA: Instrum. Soc. Amer., 1995.

[2] A. O'Dwyer, *Handbook of PI and PID Controller Tuning Rules*, 3rd ed. London, U.K.: Imperial College Press, 2009.

[3] L. Desborough and R. Miller, "Increasing customer value of industrial control performance monitoring-Honeywell's experience," in *Proc. 6th Int. Conf. Chem. Process Control*, vol. 98. New York, NY, USA: Amer. Inst. Chem. Eng., 2002, pp. 169–189.

[4] H. Wu, W. Su, and Z. Liu, "PID controllers: Design and tuning methods," in *Proc. 9th IEEE Conf. Ind. Electron. Appl.*, Hangzhou, China, Jun. 2014, pp. 808–813.

[5] *What is the Percentage of the PID Algorithm Applications in Industry?*. Accessed: May 23, 2022. [Online]. Available: https://www.researchgate.net/post/What_is_the_percentage_of_the_PID_algorithm_applications_in_industry

[6] S. P. Bhattacharyya, "Robust control under parametric uncertainty: An overview and recent results," *Annu. Rev. Control*, vol. 44, pp. 45–77, Jan. 2017.

[7] S. P. Bhattacharyya, A. Datta, and L. H. Keel, *Linear Control Theory: Structure, Robustness, and Optimization*. Boca Raton, FL, USA: CRC Press, 2009.

[8] Y. I. Neimark, "Search for the parameter values that make automatic control system stable," *Automatika Telemehanika*, vol. 9, no. 3, pp. 190–203, 1948.

[9] D. Mitrović, "Graphical analysis and synthesis of feedback control systems: I-theory and analysis; II-synthesis; III-sampled-data feedback control systems," *Trans. Amer. Inst. Electr. Eng., II, Appl. Ind.*, vol. 77, no. 6, pp. 476–503, 1959.

[10] D. D. Šiljak, "Analysis and synthesis of feedback control systems in the parameter plane: I-linear continuous systems; II-sampled-data systems; III-nonlinear systems," *Trans. Amer. Inst. Electr. Eng., II, Appl. Ind.*, vol. 83, no. 75, pp. 449–473, 1964.

[11] D. D. Šiljak, "Generalization of the parameter plane method," *IEEE Trans. Autom. Control*, vol. AC-11, no. 1, pp. 63–70, Jan. 1966.

[12] J. Ackermann, *Robust Control: The Parameter Space Approach*. London, U.K.: Springer, 2002.

[13] E. N. Gryazina and B. T. Polyak, "Stability regions in the parameter space: *D*-decomposition revisited," *Automatica*, vol. 42, no. 1, pp. 13–26, Jan. 2006.

[14] B. N. Le, Q.-G. Wang, and T. H. Lee, "Development of D-decomposition method for computing stabilizing gain ranges for general delay systems," *J. Process Control*, vol. 25, pp. 94–104, Jan. 2015.

[15] P. D. Mandić, T. B. Šekara, M. P. Lazarević, and M. Bošković, "Dominant pole placement with fractional order PID controllers: D-decomposition approach," *ISA Trans.*, vol. 67, pp. 76–86, Mar. 2017.

[16] N. Bajcinca, "Design of robust PID controllers using decoupling at singular frequencies," *Automatica*, vol. 42, no. 11, pp. 1943–1949, Nov. 2006.

[17] M.-T. Ho, A. Datta, and S. P. Bhattacharyya, "A new approach to feedback stabilization," in *Proc. 35th IEEE Conf. Decis. Control*, Kobe, Japan, 1996, pp. 4643–4648.

[18] N. Tan and I. Kaya, "Computation of stabilizing PI controllers for interval systems," in *Proc. 11th Medit. Conf. Control Automat.*, Rhodes, Greece, 2003, pp. 1–6.

[19] N. Tan, I. Kaya, C. Yeroglu, and D. P. Atherton, "Computation of stabilizing PI and PID controllers using the stability boundary locus," *Energy Convers. Manage.*, vol. 47, no. 18, pp. 3045–3058, Nov. 2006.

[20] M. T. Söylemez, N. Munro, and H. Baki, "Fast calculation of stabilizing PID controllers," *Automatica*, vol. 39, no. 1, pp. 121–126, Jan. 2003.

[21] J. Fang, D. Zheng, and Z. Ren, "Computation of stabilizing PI and PID controllers by using Kronecker summation method," *Energy Convers. Manage.*, vol. 50, no. 7, pp. 1821–1827, Jul. 2009.

[22] E. Almodaresi and M. Bozorg, "k_p-stable regions in the space of time delay and PI controller coefficients," *Int. J. Control*, vol. 88, no. 3, pp. 653–662, Mar. 2015.

[23] E. Almodaresi and M. Bozorg, "K_P-stable regions in the space of PID controller coefficients," *IET Control Theory Appl.*, vol. 11, no. 10, pp. 1642–1647, Jun. 2017.

[24] İ. Mutlu, F. Schrödel, N. Bajcinca, D. Abel, and M. T. Söylemez, "Lyapunov equation based stability mapping approach: A MIMO case study," *IFAC-PapersOnLine*, vol. 49, no. 9, pp. 130–135, 2016.

[25] N. Hohenbichler, "All stabilizing PID controllers for time delay systems," *Automatica*, vol. 45, no. 11, pp. 2678–2684, Nov. 2009.

[26] N. Bajcinca, "Computation of stable regions in PID parameter space for time delay systems," in *Proc. 5th IFAC Workshop Time-Delay Syst.*, Leuven, Belgium, 2004, pp. 1–6.

[27] I. Kaya and S. Atic, "PI controller design based on generalized stability boundary locus," in *Proc. 20th Int. Conf. Syst. Theory, Control Comput. (ICSTCC)*, Sinaia, Romania, Oct. 2016, pp. 24–28.

[28] S. Atic and I. Kaya, "PID controller design based on generalized stability boundary locus to control unstable processes with dead time," in *Proc. 26th Medit. Conf. Control Autom. (MED)*, Zadar, Croatia, Jun. 2018, pp. 1–6.

[29] S. Atic, E. Cokmez, F. Peker, and I. Kaya, "PID controller design for controlling integrating processes with dead time using generalized stability boundary locus," *IFAC-PapersOnLine*, vol. 51, no. 4, pp. 924–929, 2018.

[30] F. Schrödel, S. K. Manickavasagam, and D. Abel, "A comparative overview of different approaches for calculating the set of all stabilizing PID controller parameters," *IFAC-PapersOnLine*, vol. 48, no. 14, pp. 43–49, 2015.

[31] I. Mutlu, F. Schrodel, D. Mihailescu-Stoica, K. Alaa, and M. T. Soylemez, "A case study on determining stability boundaries of parameter uncertain systems," in *Proc. 26th Medit. Conf. Control Autom. (MED)*, Zadar, Croatia, Jun. 2018, pp. 1–9.

[32] K. Alaa, I. Mutlu, F. Schrodel, D. Mihailescu-Stoica, and R. Vosswinkel, "A combined approach to determine robustly stabilizing parameter spaces," in *Proc. 27th Medit. Conf. Control Autom. (MED)*, Akko, Israel, Jul. 2019, pp. 106–111.

[33] B. R. Barmish, C. V. Hollot, F. J. Kraus, and R. Tempo, "Extreme point results for robust stabilization of interval plants with first-order compensators," *IEEE Trans. Autom. Control*, vol. 37, no. 6, pp. 707–714, Jun. 1992.

[34] B. R. Barmish, *New Tools for Robustness of Linear Systems*. New York, NY, USA: Macmillan, 1994.

[35] R. Matušů and R. Prokop, "Computation of robustly stabilizing PID controllers for interval systems," *SpringerPlus*, vol. 5, no. 1, pp. 1–15, Dec. 2016, doi: 10.1186/s40064016-2341-z.

[36] H. Chapellat and S. P. Bhattacharyya, "A generalization of Kharitonov's theorem; robust stability of interval plants," *IEEE Trans. Autom. Control*, vol. 34, no. 3, pp. 306–311, Mar. 1989.

[37] Y. J. Huang and Y.-J. Wang, "Robust PID tuning strategy for uncertain plants based on the Kharitonov theorem," *ISA Trans.*, vol. 39, no. 4, pp. 419–431, Sep. 2000.

[38] C. Yeroglu and N. Tan, "Design of robust PI controller for vehicle suspension system," *J. Electr. Eng. Technol.*, vol. 3, no. 1, pp. 135–142, Mar. 2008.

[39] I. D. Diaz-Rodriguez and S. P. Bhattacharyya, "PI controller design in the achievable gain-phase margin plane," in *Proc. IEEE 55th Conf. Decis. Control (CDC)*, Las Vegas, NV, USA, Dec. 2016, pp. 4919–4924.

[40] T. Bünte, "Mapping of Nyquist/Popov theta-stability margins into parameter space," *IFAC-PapersOnLine*, vol. 33, no. 14, pp. 519–524, 2000.

[41] D. Odenthal and P. Blue, "Mapping of frequency response performance specifications into parameter space," *IFAC-PapersOnLine*, vol. 33, no. 14, pp. 531–536, 2000.

[42] L. Pyta, R. Vobwinkel, F. Schrodel, N. Bajcinca, and D. Abel, "Parameter space approach for performance mapping using Lyapunov stability," in *Proc. 26th Medit. Conf. Control Autom. (MED)*, Zadar, Croatia, Jun. 2018, pp. 1–9.

[43] R. Voßwinkel, L. Pyta, F. Schrödel, İ. Mutlu, D. Mihailescu-Stoica, and N. Bajcinca, "Performance boundary mapping for continuous and discrete time linear systems," *Automatica*, vol. 107, pp. 272–280, Sep. 2019.

[44] Y. J. Wang, "Graphical computation of gain and phase margin specifications-oriented robust PID controllers for uncertain systems with time-varying delay," *J. Process Control*, vol. 21, no. 4, pp. 475–488, Apr. 2011.

[45] X.-W. Zhao and J.-Y. Ren, "Computation of PID stabilizing region with stabilized margins," *Opt. Precis. Eng.*, vol. 21, no. 12, pp. 3214–3222, 2013.

[46] Y.-J. Wang, S.-T. Huang, and K.-H. You, "Calculation of robust and optimal fractional PID controllers for time delay systems with gain margin and phase margin specifications," in *Proc. 36th Chin. Control Conf. (CCC)*, Xi'an, China, Jul. 2017, pp. 3077–3082.

[47] Y.-J. Wang, "Determination of all feasible robust PID controllers for open-loop unstable plus time delay processes with gain margin and phase margin specifications," *ISA Trans.*, vol. 53, no. 2, pp. 628–646, Mar. 2014.

[48] F. Asadi, *Robust Control of DC–DC Converters: The Kharitonov's Theorem Approach With MATLAB® Codes*. San Rafael, CA, USA: Morgan & Claypool, 2018.

[49] T. Mori and S. Barnett, "On stability tests for some classes of dynamical systems with perturbed coefficients," *IMA J. Math. Control Inf.*, vol. 5, no. 2, pp. 117–123, 1988.

[50] H. Chapellat, M. Dahleh, and S. P. Bhattacharyya, "Robust stability under structured and unstructured perturbations," *IEEE Trans. Autom. Control*, vol. 35, no. 10, pp. 1100–1108, Oct. 1990.

[51] C. V. Hollot and R. Tempo, "On the Nyquist envelope of an interval plant family," *IEEE Trans. Autom. Control*, vol. 39, no. 2, pp. 391–396, Feb. 1994.

[52] N. Tan and D. P. Atherton, "A user friendly toolbox for the analysis of interval systems," in *Proc. 3rd IFAC Symp. Robust Control Design*, Prague, Czech Republic, 2000, pp. 501–506.

[53] N. Sayyaf and M. S. Tavazoei, "Frequency data-based procedure to adjust gain and phase margins and guarantee the uniqueness of crossover frequencies," *IEEE Trans. Ind. Electron.*, vol. 67, no. 3, pp. 2176–2185, Mar. 2020.

[54] R. Matusu, B. Senol, and L. Pekar, "Robust PI control of interval plants with gain and phase margin specifications: Application to a continuous stirred tank reactor," *IEEE Access*, vol. 8, pp. 145372–145380, 2020.

[55] R. C. Dorf, *Modern Control Systems*. Reading, MA, USA: Addison-Wesley, 1974.

[56] V. L. Kharitonov, "Asymptotic stability of an equilibrium position of a family of systems of linear differential equations," *Differentsial'nye Uravneniya*, vol. 14, pp. 2086–2088, Jan. 1978.

[57] K. Zhou, J. C. Doyle, and K. Glover, *Robust and Optimal Control*. Upper Saddle River, NJ, USA: Prentice-Hall, 1996.

[58] M. Šebek and Z. Hurák, "An often missed detail: Formula relating peek sensitivity with gain margin less than one," in *Proc. 17th Int. Conf. Process Control*, Štrbské Pleso, Slovakia, 2009, pp. 65–72.

RADEK MATUŠŮ was born in Zlín, Czech Republic, in 1978. He received the M.S. degree in automation and control technology in consumer goods industry from the Faculty of Technology, Tomas Bata University (TBU) in Zlín, in 2002, and the Ph.D. degree in technical cybernetics from the Faculty of Applied Informatics (FAI), TBU in Zlín, in 2007.

He has been holding various research or pedagogical positions at TBU in Zlín, since 2004, where he is currently a Researcher and a Project Manager. He was appointed as an Associate Professor of machine and process control at the FAI, TBU in Zlín, in 2018. He has (co)authored more than 50 scientific journal articles and over 110 conference contributions. His research interests include analysis and synthesis of robust control systems, fractional-order systems, and algebraic methods in control design.

Prof. Matušů is a member of the Topical Advisory Panel. He serves as an Academic Editor for the *Journal of Control Science and Engineering*. He was a Guest Editor of *Mathematic Problems in Engineering*. He has also served as a Reviewer for over 50 scientific journals, including *Automatica*, IEEE TRANSACTIONS ON AUTOMATIC CONTROL, and *IEEE Control Systems Magazine*.

BILAL ŞENOL received the B.S. and M.S. degrees in electrical and electronics engineering and the Ph.D. degree in computer engineering from İnönü University, Malatya, Turkey, in 2009, 2011, and 2015, respectively.

He is currently working as an Associate Professor with the Computer Engineering Department. His research interests include fractional order analysis and controller design. He also has works related to computer aided design and user friendly interfaces for system analysis.

BARIS BAYKANT ALAGOZ received the bachelor's degree in electronics and communication engineering from Istanbul Technical University, in 1998, and the Ph.D. degree in electrical electronics engineering from Inonu University, in 2015. His research interests include modeling and simulation, control systems, computational intelligence, intelligent systems, and smart grids.

LIBOR PEKAŘ was born in Zlín, Czech Republic, in 1979. He received the B.S. degree in automation and informatics, the M.S. degree in automation and control engineering in consumption industries, and the Ph.D. degree in technical cybernetics from Tomas Bata University in Zlín, Czech Republic, in 2002, 2005, and 2013, respectively.

From 2006 to 2013, he worked at the university as a Junior Lecturer, where he became a Senior Lecturer, in 2013, and was appointed as an Associate Professor, in 2018. He is currently an Associate Professor at the Faculty of Applied Informatics, Tomas Bata University in Zlín. He is the author of one book and eight book chapters, more than 45 journal articles, and 70 conference papers. His research interests include analysis, modeling, identification, and control of time-delay systems, algebraic control methods, autotuning, and optimization techniques.

Prof. Pekař received the Laureate of the ASR Seminary Instrumentation and Control in 2007 and 2009, and the Rectors' Award for the Best Ph.D. Thesis in the Faculty of Applied Informatics, Tomas Bata University, in 2013. He served as the Lead Guest Editor for special issues in *Advances in Mechanical Engineering* journal and *Mathematics* journal, and as the Guest Editor for a special collection in *Frontiers in Energy Research* journal. He has been an Editor of *Mathematical Problems in Engineering*, since 2018, and *AppliedMath* journal, since 2022. He has served as a Reviewer for contributions to many highly regarded journals, such as *Applied Mathematics and Computations*, *Automatica*, *ESAIM: Control, Optimisation and Calculus of Variations*, the IEEE TRANSACTIONS ON AUTOMATIC CONTROL, the IEEE TRANSACTIONS ON INDUSTRIAL ELECTRONICS, *International Journal of Control*, *International Journal of Robust and Nonlinear Control*, *Systems & Control Letters*, *Swarm and Evolutionary Computation*, and many others.